

CHAPTER 5

PHASE TRANSITIONS IN SOME Cu^+ ION CONDUCTING
SOLID ELECTROLYTES

INTRODUCTION

Ionic solids are able to transport charge due to the movement of ions. Their ionic conductivity varies over an extremely large range, from that of very good insulators to that of good conductors ($\sim 1 \Omega^{-1} \text{ cm}^{-1}$). Because the migration of ions through crystals requires thermally activated processes, the ionic conductivity increases significantly with temperature. However, all compounds exhibiting this ion transport property in the solid state should not be termed as solid electrolytes. In fact, in many of them, electrolytic conductivity arises due to the equilibrium concentration of point defects; that is, the conductivity results from annihilation and creation of defects that would not be present if the crystals were ideally perfect. At room temperature specific conductivity of these compounds lie in the range $\sim 10^{-6} - 10^{-12} \Omega^{-1} \text{ cm}^{-1}$.

Ionic conductivity in a true solid electrolyte is an inherent property of the material and is directly related to its crystal structure. From structural studies of a number of solid electrolytes it has emerged that the two primary structural characteristics of true solid electrolytes are^{1,2}: (i) A large ratio of crystallographic sites available to the mobile cations to the available number of mobile cations. (ii) Networks of

pathways resulting from the face-sharing of anion polyhedra. The networks are different in detail in different structures, but those having simpler three-dimensional networks are expected to have higher bulk conductivities. In an anisotropic solid electrolyte, the highest conductivity is in the direction of simplest pathways^{1,2}.

Table 5.1 summarizes the structural and phase transitional aspects of some AgI-based solid electrolytes. The relation between the sites available in the unit cell to the number of mobile ions present and the electrical conductivity for some of these solid electrolytes is shown in Table 5.2.

The replacement of Ag⁺ ion by Cu⁺ ion in solid electrolytes is of both scientific and practical interest. Inasmuch as both silver(I) and copper(I) prefer to have tetrahedral or three-coordinated environment one can expect to find solid electrolytes of related structures. However, there is significant difference in the sizes of the two ions, and that probably is the reason why there are very few Cu⁺ ion solid electrolytes that are isostructural with Ag⁺ ion solid electrolytes.

Until recently the solid electrolyte with highest room temperature conductivity was RbAg₄I₅, with $\sigma = 0.27 \Omega^{-1} \text{cm}^{-1}$. The high conductivity is a sequel to its open structure.

Table 5.1

Structural aspects and phase transitions of AgI- based
solid electrolytes

Compound	Comments	Reference
AgI	There are three phases for AgI; $\beta \rightarrow \alpha$ transition occurs at 146°C ; α -phase is solid electrolyte. α -AgI is cubic, space group $\text{Im } 3\text{m}$; anion arrangement is bcc.	3-5
Ag ₃ SI, Ag ₃ SBr	Ag ₃ SI undergoes transition ($\beta \rightarrow \alpha$) at 235°C . The anion arrangement in α -Ag ₃ SI is bcc but in β -Ag ₃ SI and Ag ₃ SBr it is CsCl type.	6,7
α -Ag ₂ HgI ₄	The phase transition occurs at 50°C . The α -phase is cubic with fcc anion arrangement.	8,9
RbAg ₄ I ₅ , NH ₄ Ag ₄ I ₅ , (K _{0.5} Rb _{0.5})Ag ₄ I ₅	Three different phases (γ, β, α) exist with increase in temperature. The α - phase is cubic and highly conducting. See text for details.	10-16

contd..

Table 5.1 (contd)

Compound	Comments	Reference
$[(\text{CH}_3)_4\text{N}] \text{Ag}_{13}\text{I}_{15}$	Rhombohedral, space group $R_{32}(D_3^7)$. Full structure determination has been made. No phase change observed down to 220K.	17,18
pyAg_5I_6 (py = pyridinium ion)	Probably four crystallographic forms exists. The β -phase is hexagonal with space group $P6/mcc(D_{6h}^2)$; complete structural analysis has been made at -30°C . The $\alpha - \beta$ transition occurs at 325K; $\beta \rightarrow \sqrt{}$ at 230K; $\sqrt{} \rightarrow \delta$ at 180K.	19-22
$\text{py}_5\text{Ag}_{18}\text{I}_{23}$	The trigonal cell has the space group $P\bar{6}2m$; structure determination has been made. It is a two-dimensional solid electrolyte.	23,24
$\text{Ag}_{26}\text{I}_{18}\text{W}_4\text{O}_{16}$	Monoclinic, space group $C2(C_2^3)$; complete structural analysis has been made. Three phases exist; $\alpha \rightarrow \beta$ at 246K and $\beta \rightarrow \sqrt{}$ at 197K.	25-27

Table 5.2

Structure conductivity correlation in some AgI-based solid electrolytes^{2,28}

Compound	Ag ⁺ ions/ unit cell	Ag ⁺ ion sites/ unit cell	Vol. of channels/ Vol. of unit cell	$\sigma \Omega^{-1} \text{ cm}^{-1}$	296K	419K
-AgI	2	12	1.00			1.3
HbAg ₄ I ₅	16	56	0.471		0.27	0.66
PVAg ₅ I ₆	10	34	0.525		0.077	1.1
(CH ₃) ₄ N ₂ Ag ₁₃ I ₁₅	13	41	0.39		0.04	0.26
Ag ₂₆ I ₁₈ W ₄ O ₆	23.2	90 ^a + 56 ^b	0.344 ^a + 0.221 ^b		0.058 ^c 0.097 ^d	0.31
PV ₅ Ag ₁₈ I ₂₃	18	55	0.316		0.008	0.05

^a Pure iodide polyhedra. ^b Mixed I-O polyhedra. ^c From polycrystalline material.

^d From single crystal measurement.

It can be expected that copper(I) compounds having the same structure would also exhibit very high conductivity.

There are three crystalline modifications of RbAg_4I_5 , labelled α , β , γ in order of decreasing temperature. The cubic α -form exists above 209 K, the unit cell contains 4 molecules of RbAg_4I_5 and the space group is $P4_132(O^7)$ or $P4_332(O^6)^{12}$. The 20 iodide ions form 56 face-shared tetrahedra and create a network of pathways for the diffusion of Ag^+ ions. The 16 Ag^+ ions are distributed nonuniformly over the 56 sites. Of the 56 crystallographic sites two are 24-fold (Ag(II) and Ag(III) sites) and one 8-fold (Ag(c) sites). The room temperature occupancies of these sites by Ag^+ ions are: 0.9 ± 0.3 (Ag(c)), 9.4 ± 0.9 (Ag(II)) and 5.5 ± 0.8 (Ag(III)). The migration of Ag^+ ions occur through two zigzag cross-linked channels that are perpendicular to each face of the unit cell, resulting in the diffusion to take place in three dimensions¹².

The $\alpha - \beta$ phase transformation of RbAg_4I_5 at 209K is second order^{13,15,16}. The β -phase is rhombohedral and belongs to the space group $R32(D_3^7)^{14}$. Displacement of I^- , Rb^+ ions, and Ag^+ ion sites relative to their positions in the cubic space group are small. The main difference is a redistribution of the Ag^+ ions¹⁴. It is most likely that the $\alpha - \beta$ transition is a disorder-disorder transformation.

The $\beta - \sqrt{3}$ transition occurs at 122 K¹⁵⁻¹⁷. The $\sqrt{3}$ -phase is trigonal and belongs to the space group P321¹⁴. Although the $\beta - \sqrt{3}$ transition is first-order, however, the $\sqrt{3}$ -phase is not ordered even at 90K. There are evidences to show that the $\sqrt{3}$ -phase is still a solid electrolyte^{1,2,14}.

The Rb⁺ ion in RbAg₄I₅ can be substituted by other alkali metal ions. For example, KAg₄I₅, NH₄Ag₄I₅, (K_{0.5}Rb_{0.5})Ag₄I₅ and (K_{0.75}Rb_{0.25})Ag₄I₅, (K_{0.5}Cs_{0.5})Ag₄I₅ are all solid electrolytes and isostructural with RbAg₄I₅^{10,11}. At least 20% of Ag⁺ ion in RbAg₄I₅ can be replaced by Cu⁺ at 150°C.²

During the last few years quite a good number of Cu⁺ ion conductors have been reported. However, most of them are ill-characterized compounds and structural informations are lacking. Here we shall confine our discussion only to structurally well characterized compounds.

There are two important structural features of the Cu⁺ ion conductors CuTeX (X = Cl, Br, I)^{29,30}. One main component is the infinite 4-fold tellurium helices arranged parallel to the crystallographic c-axis. A second structural building block consists of almost regular X₄ tetrahedra linked into unlimited chains along the crystallographic c-axis by sharing sides. Within the chains, there are three independent crystallographic sites for copper, all of which are statistically occupied. The room temperature conductivities of these compounds are rather low $5 \times 10^{-2} - 5 \times 10^{-3} \Omega^{-1}\text{cm}^{-1}$, however, at temperature higher

than 200°C all of them become highly conducting. CuTeBr undergoes a phase transition at 75°C³¹.

The pyridinium compound $\text{py}_2\text{Cu}_5\text{Br}_7$ is another solid electrolyte whose crystal structure has been determined^{32,33}. In the orthorhombic space group $\text{P}2_12_12_1$, 20 Cu^+ ions ($z=4$) are distributed nonuniformly over 52 tetrahedral sites. The ratio of available sites to current carriers and the percentage of unit cell volume attributable to the conduction pathways are both rather low. The average conductivity at room temperature is $1.7 \times 10^{-2} \Omega^{-1}\text{cm}^{-1}$.³³

As already mentioned for the best Cu^+ ion conductors the most likely structure would be the one related to $\alpha\text{-RbAg}_4\text{I}_5$. This has been realized in the compound $\text{RbCu}_4\text{Cl}_3\text{I}_2$ which has the space group $\text{P}4_332(0^6)$ ³⁴. As in $\alpha\text{-RbAg}_4\text{I}_5$, there are three sets of tetrahedral sites for the charge carriers with a total of 56 sites. In this compound all the tetrahedra have both Cl^- and I^- ions at apices, but the coordination polyhedron about the Rb^+ ions contain only Cl^- ions. The conduction networks in $\text{RbCu}_4\text{Cl}_3\text{I}_2$ are similar to those in RbAg_4I_5 . The fractional occupancies of the sites in $\text{RbCu}_4\text{Cl}_3\text{I}_2$ are: 0.339 (Cu(c)), 0.294 (Cu(II)) and 0.132 (Cu(III))³⁴.

It has been observed that the solid solution RbCu_4Cl_3 ($\text{I}_{2-x}\text{Cl}_x$) exists over the composition range $0 \leq x \leq 0.40$ ^{35,36}.

Unlike in RbAg_4I_5 none of the composition $\text{RbCu}_4\text{Cl}_3(\text{I}_{2-x}\text{Cl}_x)$ undergoes any phase transition down to 78K. However, cold working of the stoichiometric $\text{RbCu}_4\text{Cl}_3\text{I}_2$ causes a transition with slight decomposition to a new complex phase which is itself stable in only a narrow temperature range (0-35°C)³⁵. $\text{RbCu}_4\text{Cl}_3\text{I}_2$ is thermodynamically stable in only a narrow temperature range, $200 \pm 15^\circ\text{C}$. With just slight replacement of some I^- by Cl^- ions (x ca. 0.02), the compounds become stable between at least 78K and their preparation temperatures which depend on x . The cold-worked phase transforms to the cubic phase with the formula $\text{RbCu}_4\text{Cl}_3(\text{I}_{1.96}\text{Cl}_{0.04})$ at temperatures above 75°C. The transformation is first order. The new phase has the room temperature conductivity $1.5 \times 10^{-4} \Omega^{-1}\text{cm}^{-1}$.³⁶

Electrical conductivity has been measured as a function of temperature and composition of the system $\text{RbCu}_4\text{Cl}_3(\text{I}_{2-x}\text{Cl}_x)$ ³⁷. Room temperature conductivities decrease very nearly linearly from $0.39 \Omega^{-1}\text{cm}^{-1}$ for the stoichiometric composition to $0.28 \Omega^{-1}\text{cm}^{-1}$ for $x = 0.40$. Table 5.3 shows the trend in conductivity values. The decrease in conductivity with increasing x is caused by the disorder introduced by the replacement of iodide by chloride ions. The most important point to note here is that the solid electrolytes $\text{RbCu}_4\text{Cl}_3(\text{I}_{2-x}\text{Cl}_x)$ have the highest room temperature conductivities.

Table 5.3

Conductivity results for the $\text{RbCu}_4\text{Cl}_3(\text{I}_{2-x}\text{Cl}_x)$ system³⁷

x	σ ($\Omega^{-1} \text{cm}^{-1}$)		Enthalpy of activation of motion (eV)
	298 K	419 K	
0.00	0.39	0.97	0.112
0.10	0.36	0.90	0.112
0.14	0.34	0.85	0.112
0.20	0.33	0.83	0.114
0.27	0.31		
0.32	0.30	0.76	0.115
0.40	0.28	0.72	0.117

A new solid electrolyte with narrow solid solution range, $\text{NH}_4\text{Cu}_4\text{Cl}_3(\text{I}_{2-x}\text{Cl}_x)$, $0.09 \leq x \leq 0.13$ isostructural with RbAg_4I_5 has been reported³⁸. $\text{NH}_4\text{Cu}_4\text{Cl}_3(\text{I}_{1.9}\text{Cl}_{0.1})$ is thermodynamically stable between 130° and 170°C and has room temperature conductivity $0.21 \Omega^{-1}\text{cm}^{-1}$. Finally, KCu_4I_5 known to be stable between 257 and 332°C is also a solid electrolyte.

The purpose of the present study is to investigate thermal stability and phase transition behavior of the systems $\text{CsCu}_4\text{Cl}_3(\text{I}_{2-x}\text{Cl}_x)$ and $(\text{Cs}_{1-y}\text{Rb}_y)\text{Cu}_4\text{Cl}_3(\text{I}_{2-x}\text{Cl}_x)$.

EXPERIMENTAL SECTION

The solid electrolytes $\text{CsCu}_4\text{Cl}_3(\text{I}_{2-x}\text{Cl}_x)$ $0 \leq x \leq 0.25$ and $(\text{Cs}_{1-y}\text{Rb}_y)\text{Cu}_4\text{Cl}_3(\text{I}_{2-x}\text{Cl}_x)$ were prepared by Geller, Ray, and Nag³⁹ and were received as a gift from Professor S. Geller of Boulder, Colorado. Their method of preparation is described below.

CuCl was prepared by the method of Keller and Wycoff⁴⁰ and CuI by the method of Kauffman and Pinnel⁴¹ with modification³⁵ to remove occluded $\text{Na}_2\text{S}_2\text{O}_3$. CsCl and RbCl (cerac 99.9%) were used after drying in vacuo at $100\text{--}110^\circ\text{C}$ for 16h.

To prepare the (substituted) pseudoternary salts, appropriate amounts of CsCl, RbCl, CuCl and CuI, for a 2.1-2.4 g specimen, were ground together in an agate mortar, inside a nitrogen-recirculating glove box. The mixture was then pelletized, put into a Pyrex test tube which was evacuated, flushed with dry nitrogen, evacuated, and again flushed with dry nitrogen. The pressure was then reduced to 0.5 atm, the tube sealed off and heated for 2h at a temperature depending on the specimen composition : $x = 0-0.25$, $y = 0-0.7$, $205 \pm 5^\circ\text{C}$; $y = 0.75-0.85$, $190 \pm 5^\circ\text{C}$. The tube was removed from the furnace and opened in the glove box; the specimen was reground, repelletized, put into a Pyrex tube, again sealed off and heated as before. Usually six cycles sufficed to produce a single-phase specimen as ascertained by X-ray powder diffraction photography.

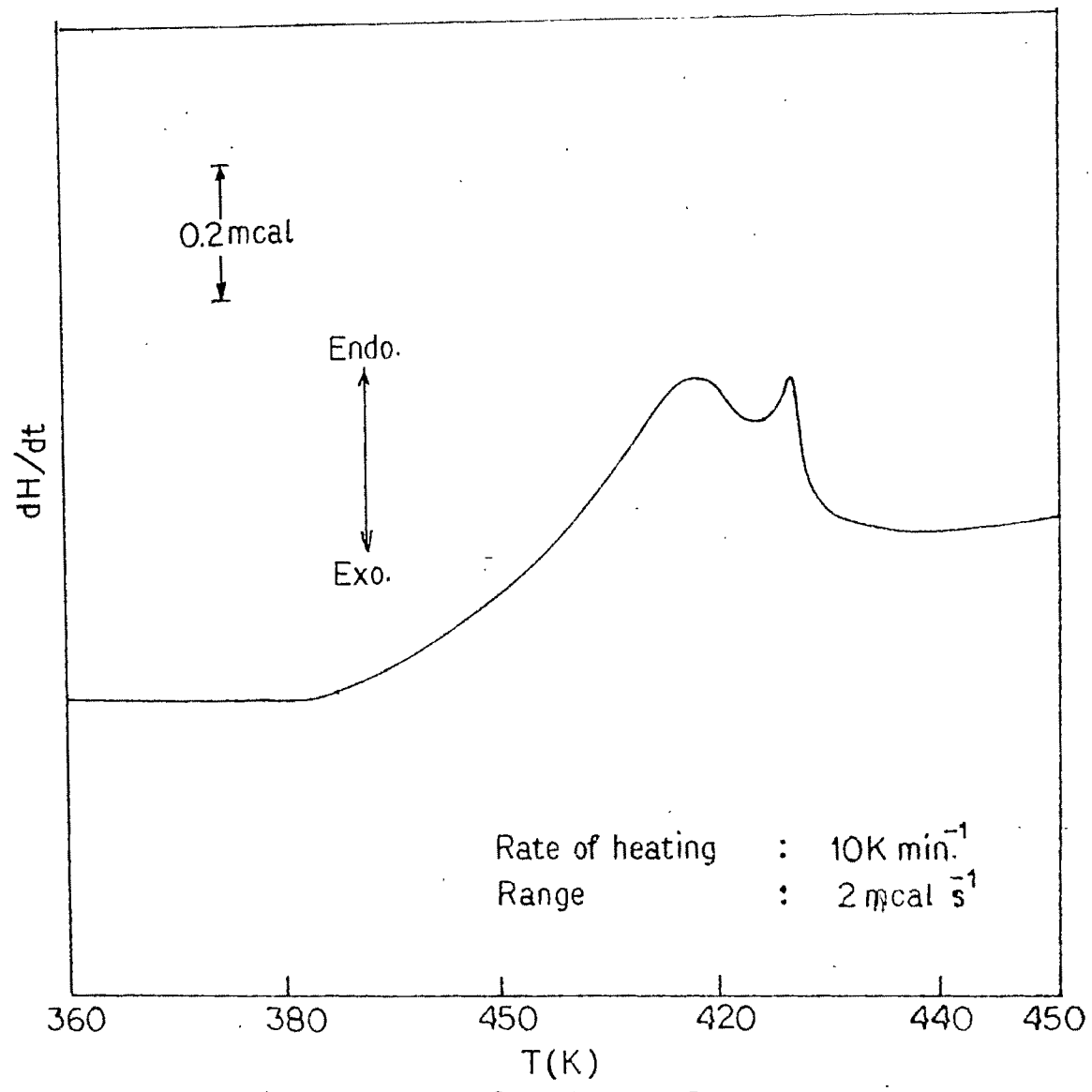
The phase transition behavior of all of the specimens were examined in a Perkin Elmer DSC-II differential scanning calorimeter. The specimens used for thermal studies were all one month old and X-ray powder photograph revealed they are the lowest temperature phase ($\sqrt{}$ -phase). Prior to the thermal analysis the sealed tube was broken, a portion of the pellet was taken and the remaining specimen was again sealed under nitrogen atmosphere. The broken specimen was quickly pulverized in an agate mortar and pestle, requisite amount of material (5-15 mg) weighed and quickly sealed into an aluminium sample holder

by crimping. Heating and cooling cycles were carried out in dry nitrogen atmosphere. The use of a gold pan sample holder demonstrated that aluminium has no detectable reactivity with the materials. The rate of heating was $10^{\circ}\text{C}/\text{min}$, and the instrument sensitivity in most of the cases was maintained to 5 mcal/s.

RESULTS AND DISCUSSION

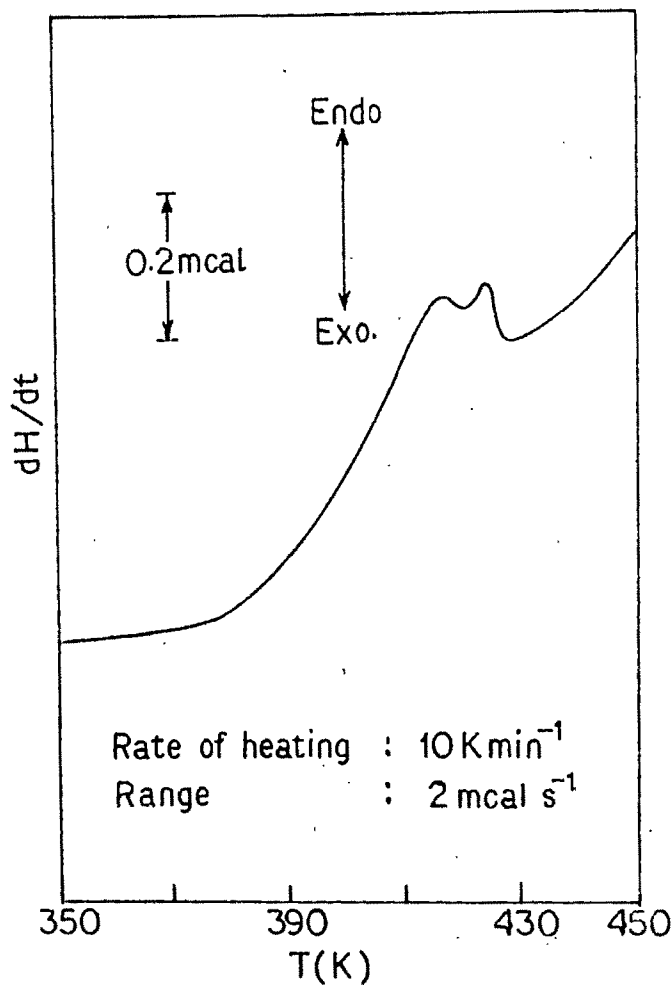
Typical DSC thermograms of the compounds $\text{Cs}_{1-y}\text{Rb}_y\text{Cu}_4\text{Cl}_3\text{I}_2$ are shown in Figures 5.1-5.7. It may be noted that the thermograms fall clearly into two categories. The compositions with lower values of y (0-0.2) show two overlapping endotherms, while the compositions with higher values of y (0.4-0.7) are marked by a single endotherm. In the compositional range $0.2 < y < 0.4$ the switch over of the double endotherms to a single endotherm take place. The transition temperatures obtained from the DSC experiments are listed in Table 5.4.

The thermal behavior of these compounds suffered from two difficulties. In spite of our best effort it was difficult to establish a base line after the phase transition was complete. For example in the case with $\text{CsCu}_4\text{Cl}_3\text{I}_2$ (Figure 5.1) it may be noted that heat is still being absorbed between 430K and 460K.



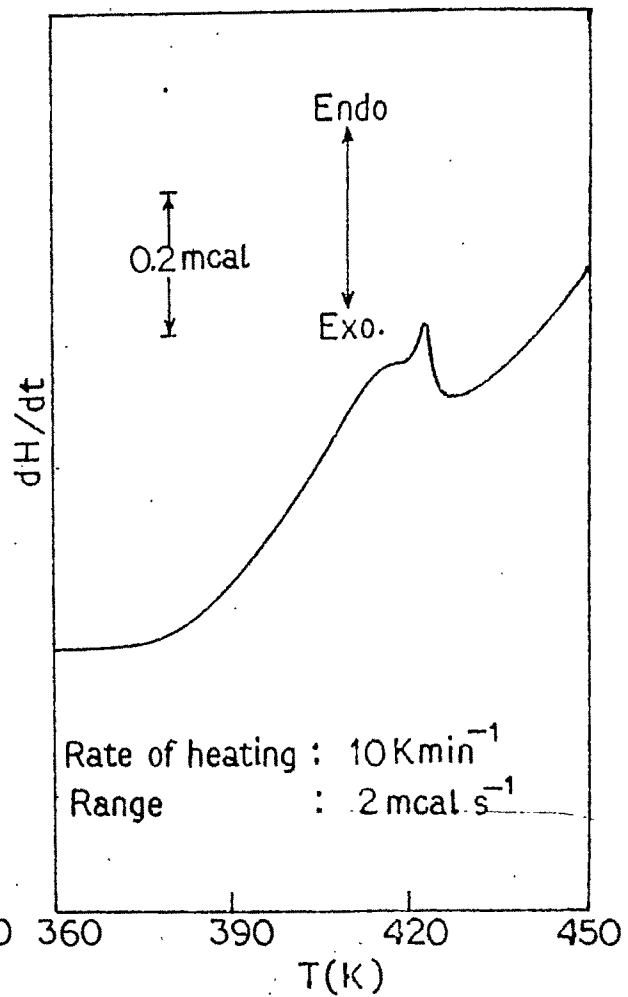
DSC scan of $\text{CsCu}_4\text{Cl}_3\text{I}_2$

Figure 5.1



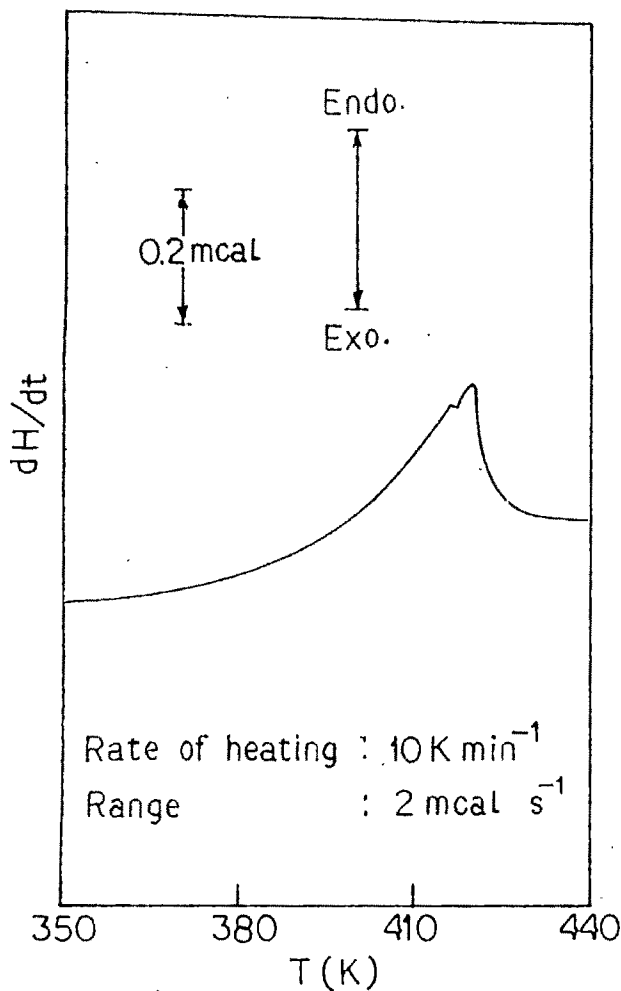
DSC scan of $\text{Cs}_{0.95}\text{Rb}_{0.05}\text{Cu}_4\text{Cl}_3\text{I}_2$

Figure. 5.2



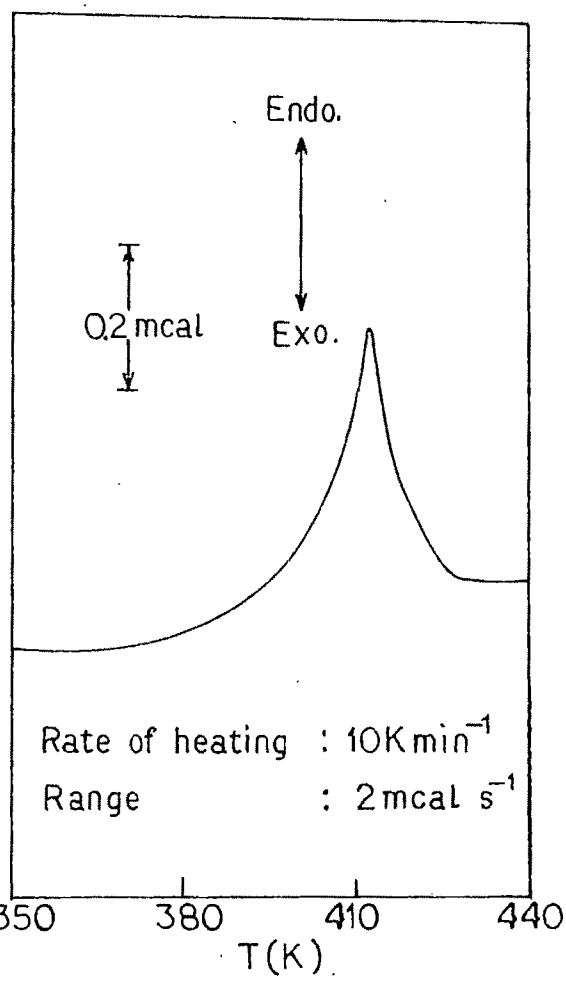
DSC scan of $\text{Cs}_{0.9}\text{Rb}_{0.1}\text{Cu}_4\text{Cl}_3\text{I}_2$

Fig. 5.3



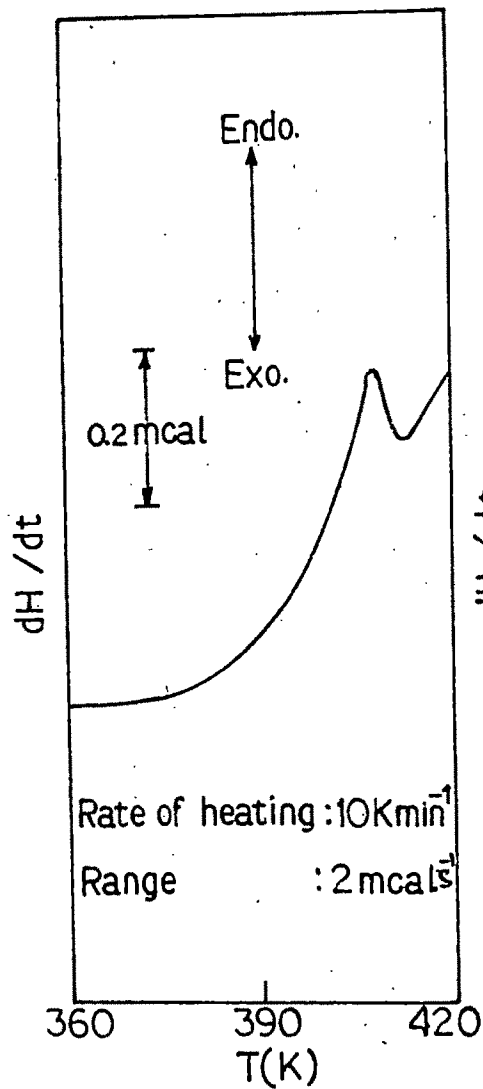
DSC scan of $\text{Cs}_{0.8}\text{Rb}_{0.2}\text{Cu}_4\text{Cl}_3\text{I}_2$

Figure 5.4

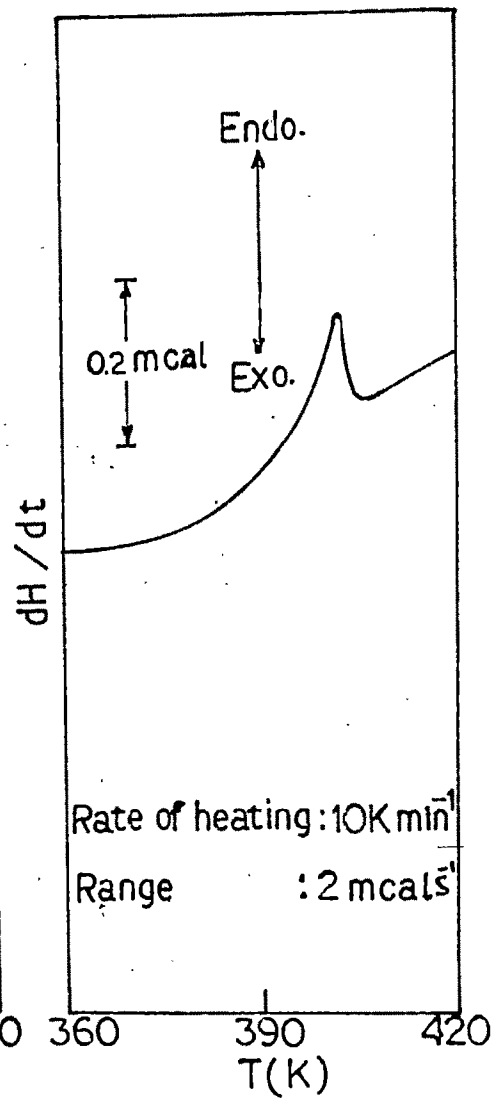


DSC scan of $\text{Cs}_{0.6}\text{Rb}_{0.4}\text{Cu}_4\text{Cl}_3\text{I}_2$

Figure 5.5



DSC scan of
 $\text{Cs}_{0.5}\text{Rb}_{0.5}\text{Cu}_4\text{Cl}_3\text{I}_2$
 Figure 5.6



DSC scan of
 $\text{Cs}_{0.3}\text{Rb}_{0.7}\text{Cu}_4\text{Cl}_3\text{I}_2$
 Figure 5.7

Table 5.4

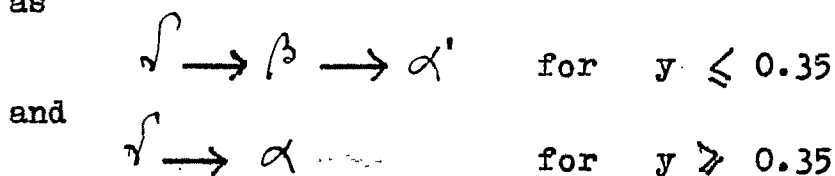
Transition temperatures of the $\text{Cs}_{1-y}\text{Rb}_y\text{Cu}_4\text{Cl}_3\text{I}_2$
system

y	Transition temperature (K)		
	$\rightarrow \beta$	$\beta \rightarrow \alpha'$	$\gamma \rightarrow \alpha$
0.00	417	427	
0.05	416	424	
0.10	415	422	
0.20	416	419	
0.30	415	417	
0.35	415	415	
0.40			412
0.50			408
0.70			402

to the lower one is extremely sluggish. It has been observed that after 16h conversion to the $\sqrt{}$ -phase was complete.

The identification of all of the phases have been made by Geller et al.³⁹ The $\sqrt{}$ -phase is orthorhombic, the unit cell dimensions for $\sqrt{}$ -CsCu₄Cl₃I₂ is $a = 14.242 \overset{\circ}{\text{A}}$, $b = 24.984 \overset{\circ}{\text{A}}$, $c = 11.712 \overset{\circ}{\text{A}}$ ⁴². This phase is isomorphous to the "cold-worked" phase of RbCu₄Cl₃I₂³⁵ (see introduction). The cell dimensions observed for RbCu₄Cl₃(I_{1.96}Cl_{0.04}) is $a = 13.908 \overset{\circ}{\text{A}}$, $b = 24.752 \overset{\circ}{\text{A}}$, $c = 11.664 \overset{\circ}{\text{A}}$ ⁴². X-ray powder data revealed that irrespective of composition the highest temperature phase is cubic. However, from single crystal measurements it has been shown³⁹ that for the compositions $0 \leq y \leq 0.35$ the α -phase has the space group P2₁3, and for $0.35 \leq y \leq 1$ the space group is P4₁32/P4₃32. It may be noted that α -RbAg₄I₅ has the space group P4₁32/P4₃32. Thus to avoid confusion we designate the cubic phase for the composition $0 \leq y \leq 0.35$ as α' and $0.35 \leq y \leq 1$ as α . The point to note here is that the space group P2₁3 is a subgroup of P4₁32 and P4₃32. The cubic phases α and α' cannot be distinguished from their powder patterns.

The β -phase which has very narrow range of thermal stability is rhombohedral. It has the space group R₃³⁹. Thus the phase transition behavior of Cs_{1-y}Cu₄Cl₃I₂ may be summarized as

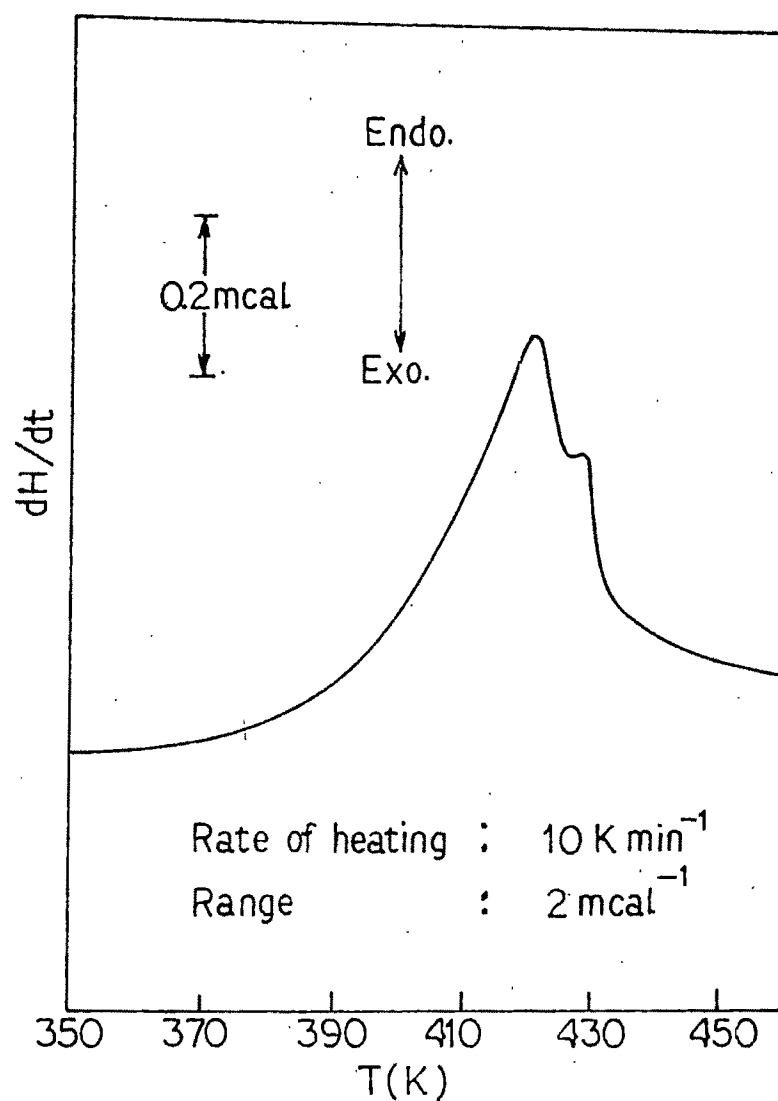


The triple point is at $y = 0.35$ and $T = 415$ K. The $\sqrt{} - \beta$, $\beta - \alpha'$ and $\sqrt{} - \alpha$ transitions are all hysteretic and therefore first order.

In the β -phase the Cu^+ ions appear to be ordered which would mean that $\beta \rightarrow \alpha'$ transformation will be order-disorder type. This is in contrast with the behavior of RbAg_4I_5 in which $\alpha - \beta$ transition is continuous and involves disorder-disorder transition (vide introduction).

Figure 5.8 shows the DSC thermogram for $\text{CsCu}_4\text{Cl}_3(\text{I}_{1.835}\text{Cl}_{0.165})$ which is typical of $\text{CsCu}_4\text{Cl}_3(\text{I}_{2-x}\text{Cl}_x)$ compounds. The phase transition behavior of these compounds are similar to $\text{Cs}_{1-y}\text{Rb}_y\text{Cu}_4\text{Cl}_3\text{I}_2$ ($0 \leq y \leq 0.35$). Table 5.5 summarizes the transition temperatures observed for the solid solutions $\text{CsCu}_4\text{Cl}_3(\text{I}_{2-x}\text{Cl}_x)$ $0 \leq x \leq 0.25$. It may be noted that both $\sqrt{} \rightarrow \beta$ and $\beta \rightarrow \alpha'$ transition temperatures remain practically invariant with the change in composition.

The combined enthalpy changes for $\sqrt{} \rightarrow \beta$ and $\beta \rightarrow \alpha'$ as well as $\sqrt{} \rightarrow \alpha$ transitions for the solid electrolyte systems $\text{Cs}_{1-y}\text{Rb}_y\text{Cu}_4\text{Cl}_3\text{I}_2$ and $\text{CsCu}_4\text{Cl}_3(\text{I}_{2-x}\text{Cl}_x)$ are collected in Table 5.6. For $\sqrt{} \rightarrow \beta \rightarrow \alpha'$ transitions ΔH values monotonically decrease with the increase in rubidium content of the compounds. When only $\sqrt{} \rightarrow \alpha$ transformation takes place, the enthalpy change again decreases as y increases. This trend is



DSC scan of $\text{CsCu}_4\text{Cl}_{3.165}\text{I}_{1.835}$

Figure 5.8

Table 5.5

Transition temperatures of the $\text{CsCu}_4\text{Cl}_3(\text{I}_{2-x}\text{Cl}_x)$ system

x	Transition temperatures (K)	
	$\gamma \rightarrow \beta$	$\beta \rightarrow \alpha'$
0.00	417	427
0.167	420	428
0.25	422	429

Table 5.6

Enthalpy changes of the systems $\text{Cs}_{1-y}\text{Rb}_y\text{Cu}_4\text{Cl}_3\text{I}_2$
and $\text{CsCu}_4\text{Cl}_3(\text{I}_{2-x}\text{Cl}_x)$

Compound	ΔH (kcal mol ⁻¹) $\sqrt{} \rightarrow \beta \rightarrow \alpha'$ or $\sqrt{} \rightarrow \alpha$
$\text{CsCu}_4\text{Cl}_3\text{I}_2$	3.2 ^a
$\text{Cs}_{0.95}\text{Rb}_{0.05}\text{Cu}_4\text{Cl}_3\text{I}_2$	3.2 ^a
$\text{Cs}_{0.9}\text{Rb}_{0.1}\text{Cu}_4\text{Cl}_3\text{I}_2$	3.1 ^a
$\text{Cs}_{0.8}\text{Rb}_{0.2}\text{Cu}_4\text{Cl}_3\text{I}_2$	2.9 ^a
$\text{Cs}_{0.7}\text{Rb}_{0.3}\text{Cu}_4\text{Cl}_3\text{I}_2$	2.7 ^a
$\text{Cs}_{0.6}\text{Rb}_{0.4}\text{Cu}_4\text{Cl}_3\text{I}_2$	1.4 ^b
$\text{Cs}_{0.5}\text{Rb}_{0.5}\text{Cu}_4\text{Cl}_3\text{I}_2$	1.0 ^b
$\text{Cs}_{0.3}\text{Rb}_{0.7}\text{Cu}_4\text{Cl}_3\text{I}_2$	0.65 ^b
$\text{CsCu}_4\text{Cl}_3(\text{I}_{1.865}\text{Cl}_{0.165})$	2.7 ^a
$\text{CsCu}_4\text{Cl}_3(\text{I}_{1.8}\text{Cl}_{0.2})$	2.6 ^a

a $\Delta H = \Delta H_{\sqrt{} \rightarrow \beta} + \Delta H_{\beta \rightarrow \alpha'}$

b $\Delta H = \Delta H_{\sqrt{} \rightarrow \alpha}$

rather expected because with the increase in cesium ion content the unit cell increases, therefore, greater thermal energy would be required for a first order phase transition to take place. In the composition $\text{CsCu}_4\text{Cl}_3(\text{I}_{2-x}\text{Cl}_x)$ limited data is available to draw a meaningful conclusion. The observed trend is, the composition richer in chloride ion shows minimum enthalpy change. In cubic $\text{RbCu}_4\text{Cl}_3\text{I}_2$ it has been shown that the rubidium ions are surrounded octahedrally only by the chloride ions. On this basis lower H for a composition with greater x is justified.

Finally it may be said that the α and α' phases are the true solid electrolytes. Extensive conductivity measurements of these systems have been made by Geller et al.³⁹ Suffice it would be to say here that the room temperature conductivity of the $\sqrt{}$ -phase is ca. $10^{-3} \Omega^{-1}\text{cm}^{-1}$, at 419K the α -phase is ca. $0.75 \Omega^{-1}\text{cm}^{-1}$ and the enthalpy of activation of motion is 0.11 eV.

REFERENCES

1. S. Geller, *Acc. Chem. Res.*, 11, 87 (1978).
2. S. Geller, in "Solid Electrolytes", Springer-Verlag, Berlin (1977).
3. L.W. Strock, *Z. Physik. Chem.*, B25, 441 (1934); B31, 132 (1936).
4. W. Buhner and W. Halg, *Helv. Phys. Acta*, 47, 27 (1974).
5. R.M. Cava and B.J. Wuensch, in "Superionic Conductors", ed. G.D. Mahan and W.L. Roth, Plenum Press, New York, p.217 (1976).
6. B. Reuter and K. Hardel, *Z. Anorg. Allg. Chem.*, 340, 158, 168 (1965).
7. B. Reuter and K. Hardel, *Ber. Bunsenges. Phys. Chem.*, 70, 82 (1966).
8. J.A.A. Ketelaar, *Z. Krist. (A)* 87, 436 (1934); *Trans. Faraday Soc.*, 34, 874 (1938).
9. J.S. Kasper and K.W. Browall, *J. Solid State Chem.*, 13, 49 (1975); 15, 54 (1975).
10. J.N. Bradley and P.D. Greene, *Trans. Faraday Soc.*, 62, 2069 (1966); 63, 424 (1967).
11. B.B. Owens and G.R. Argue, *Science*, 157, 308 (1967).

12. S. Geller, *Science*, 157, 310 (1967).
13. B.B. Owens and G.R. Argue, *J. Electrochem. Soc.*, 117, 898 (1970).
14. S. Geller, *Phys. Rev.*, B14, 4345 (1976).
15. W.V. Johnston, H. Wiedersich, and G.W. Lindberg, *J. Chem. Phys.*, 51, 3739 (1969).
16. F.L. Lederman, M.B. Salamon, and H. Peisl, *Solid State Commun.*, 19, 147 (1976).
17. B.B. Owens, *J. Electrochem. Soc.*, 117, 1536 (1970).
18. S. Geller and M.D. Lind, *J. Chem. Phys.*, 52, 5854 (1970).
19. S. Geller and B.B. Owens, *J. Phys. Chem. Solids*, 33, 1241 (1972).
20. S. Geller, *Science*, 176, 1016 (1972).
21. T. Hibma, *Phys. Rev.*, B15, 5797 (1977).
22. T. Hibma and S. Geller, *J. Solid State Chem.*, 21, 225 (1977).
23. S. Geller and P.M. Skarstad, *Phys. Rev. Lett.*, 33, 1484 (1974).
24. S. Geller, P.M. Skarstad, and S.A. Wilber, *J. Electrochem. Soc.*, 122, 332 (1975).
25. L.Y.Y. Chan and S. Geller, *J. Solid State Chem.*, 21, 331 (1977).

26. T. Takahashi, S. Ikeda, and O. Yamamoto, *J. Electrochem. Soc.*, 120, 647 (1973).
27. S. Geller, S.A. Wilber, G.F. Ruse, J.R. Akridge, and A. Turkovic, *Phys. Rev.*, B21, 2506 (1980).
28. H. Wiedersich and S. Geller, in "The Chemistry of extended defects in non-metallic solids", ed. L. Eyring and M. O'Keefe, North-Holland, Amsterdam, p. 629 (1970).
29. A. Rabenau, H. Rau, and G. Rosenstein, *Z. Anorg. Allg. Chem.*, 374, 43 (1970).
30. J. Fenner and A. Rabenau, *Z. Anorg. Allg. Chem.*, 426, 7 (1976).
31. U.V. Alpen, J. Fenner, J.D. Marcoll, and A. Rabenau, *Electrochim. Acta*, 22, 801 (1977).
32. A.F. Sammells, J.Z. Gougoutas, and B.B. Owens, *J. Electrochem. Soc.*, 122, 1291 (1975).
33. L.Y.Y. Chan, S. Geller, and P.M. Skarstad, *J. Solid State Chem.*, 25, 85 (1978).
34. S. Geller, J.R. Akridge, and S.A. Wilber, *Phys. Rev.*, B19, 5396 (1979).
35. K. Nag and S. Geller, *J. Electrochem. Soc.*, 128, 2670 (1981).

36. T. Takahashi, O. Yamamoto, S. Yamada, and S. Hayashi, J. Electrochem. Soc., 126, 1654 (1979).
37. S. Geller, K. Nag, and A.K. Ray, J. Electrochem. Soc., 128, 2675 (1981).
38. S. Geller, J.R. Akridge, and S.A. Wilber, J. Electrochem. Soc., 127, 251 (1980).
39. S. Geller, A.K. Ray, and K. Nag, unpublished work.
40. R.N. Keller and H.D. Wycoff, Inorg. Synth., 2, 1 (1946).
41. G.D. Kauffman and R.P. Pinnell, Inorg. Synth., 6, 3 (1960).
42. S. Geller, A.K. Ray, H.Z. Fardi, and K. Nag, Phys. Rev., B25, 2968 (1982).